

# Unsupervised Fuzzy C-Means Segmentation with Adaptive Cluster Count Derived from Laplacian of Gaussian Edge Maps

Dr. Rajendra Vasantrya Patil <sup>1</sup>\*, Deepak Yashwantrao Bhadane <sup>2</sup>, Dr. Abhijit Dandavate <sup>3</sup>,  
Dr. Priti Shende <sup>4</sup>, Dr. Govind Mohanlal Poddar <sup>5</sup>, Shravani R. Patil <sup>6</sup>

<sup>1</sup> Department of Computer Engineering, SSVPS Bapusaheb Shivajirao Deore College of Engineering, Dhule (MS), India

<sup>2</sup> R. C. Patel College of Engineering and Polytechnic, Shirpur (MS) • India

<sup>3</sup> Dhule Patil College of Engineering, Pune (MS) • India

<sup>4</sup> Department of Electronics and Telecommunication, Dr. D. Y. Patil Institute of Technology, Pune (MS) • India

<sup>5</sup> NES Gangamai College of Engineering, Nagaon, Dhule (MS) • India

<sup>6</sup> Department of Computer Engineering, SSVPS Bapusaheb Shivajirao Deore College of Engineering, Dhule (MS) • India

\*Corresponding author E-mail: [patilrajendra.v@gmail.com](mailto:patilrajendra.v@gmail.com)

Received: June 15, 2025, Accepted: July 11, 2025, Published: July 22, 2025

## Abstract

This paper proposes an embedded integration framework for unsupervised image segmentation that combines the strengths of edge detection and soft clustering. Traditional segmentation algorithms, such as K-means, often rely on a manually defined number of clusters (k), which can lead to inconsistent and less effective results across different images. To overcome this limitation, we introduce a Laplacian of Gaussian (LoG)-guided method that adaptively estimates the optimal number of clusters (C) based on structural edge information. The LoG operator detects zero-crossings corresponding to object boundaries, followed by edge refinement through connectivity analysis, spurious edge removal, and color-based grouping. This adaptively determined C is used as input to the Fuzzy C-Means (FCM) algorithm, which offers soft clustering with improved handling of ambiguous or gradual region boundaries. Experimental evaluations on diverse images show that the proposed LoG-FCM framework outperforms traditional K-means clustering in both visual quality and quantitative metrics. Notably, it achieves higher values in Jaccard Index, Dice Coefficient, Precision, Recall, and Adjusted Rand Index, while reducing Variation of Information and Hausdorff Distance. The results highlight the robustness, accuracy, and autonomous nature of the proposed segmentation approach.

**Keywords:** Fuzzy C-Means; Image Segmentation; Adaptive Clustering; Laplacian of Gaussian; Edge Detection; Embedded Integration; Unsupervised Learning.

## 1. Introduction

Image segmentation is a critical step in the analysis of digital images across many applications. Its main objective is to divide an image into meaningful regions that correspond to real objects or logical parts of a scene. This is similar to how children begin to recognize and separate objects in their surroundings. It helps understand the image content without requiring prior knowledge of its components. Image segmentation is used in applications such as object detection, face recognition, medical imaging, and food grain quality assessment [1], [2].

To extract useful information, it is important to distinguish foreground objects from the background. In addition to the above applications, image segmentation plays an important role in several advanced domains. These include autonomous driving (for obstacle detection and scene understanding), remote sensing (for urban planning and land cover classification), industrial inspection (for quality control and defect detection), and artistic applications such as object manipulation and style transfer [2], [3].

Image segmentation techniques are broadly categorized into several types. These include thresholding-based techniques which divide regions based on intensity values, edge-based techniques which detect discontinuities in image intensity, like the Laplacian of Gaussian or Canny, region-based techniques which cluster pixels into clusters in a feature space, and more sophisticated approaches like watershed segmentation, graph-based approaches, and deep learning-based segmentation (e.g., U-Net, Mask R-CNN) [4], [5].

Algorithms like K-means are well known for their conceptual simplicity and computational efficiency in the field of clustering-based segmentation. K-means uses hard clustering, which means each pixel belongs to only one group. This is problematic for natural images with unclear object boundaries. Fuzzy C-Means (FCM) allows pixels to belong to multiple clusters with varying degrees of membership

[6], [7]. However, both K-means and FCM require a predefined number of clusters ( $k$  or  $C$ ), which affects the quality of segmentation. Manual selection of  $k$  can lead to inconsistent results across different images and users [8].

This work presents an embedded integration approach that makes use of the Laplacian of Gaussian (LoG) operator to overcome the difficulties associated with the unsupervised calculation of ' $k$ ' for fuzzy C-Means. After Gaussian smoothing, the LoG, a second-order derivative operator, is very effective at identifying edges as zero-crossings and provides a strong reaction to abrupt changes in image intensity [9]. It is a powerful source of information for adaptively establishing the cluster count for FCM because of its capacity to generate thin, well-localized edges, which are essential for defining object boundaries.

This work's main goal is to integrate edge information from the LoG to improve the resilience and accuracy of fuzzy C-Means segmentation. This method independently predicts the ideal number of segments by combining the soft clustering capabilities of FCM with the LoG's ability to detect edges precisely. In order to achieve completely automated image analysis, our technique aims to provide an autonomous way to split input images without the need for explicit manual parameter setup. The main contribution is to improve the accuracy of FCM by using LoG-derived edge analysis to intelligently guide its segmentation process. The ultimate goal is to achieve more accurate and consistent segmentation results in complex color images, which are often difficult to segment due to varying textures and lighting conditions. To solve this problem, we present a method that uses edge detection to automatically choose the number of clusters for FCM, making the segmentation process both accurate and fully automatic.

## 2. Related work

Image segmentation has long been a key research focus in computer vision and image processing, resulting in a large and diverse body of literature. Early methods frequently concentrated on fundamental strategies like edge detection, region growth, and thresholding. Early edge detectors like Roberts, Prewitt, and Sobel worked by finding sudden changes in pixel intensity, and they laid the foundation for gradient-based edge detection [9], [10]. More advanced techniques later appeared, such as the Canny edge detector, which was praised for its stability and ability to create clean, thin edges by combining Gaussian smoothing, non-maximum suppression, and hysteresis thresholding [8], [11]. Similarly, following an initial smoothing step, the Laplacian of Gaussian (LoG) became popular for edge detection because it can find fine edges using zero-crossings and works well even in noisy images [12]. It remains relevant for modern applications where preserving edge sharpness is critical. Table 1 provides a quick comparison of these and other popular edge detection techniques.

**Table 1:** Comparison of Common Edge Detection Methods

Method	Principle	Strengths	Weaknesses	Typical Output
Roberts	Cross-gradient magnitude	Computationally simple, good for sharp edges	Highly sensitive to noise, poor localization	Thick, noisy edges
Prewitt	Averaging gradients in 3x3 mask	Robust to noise than Roberts, simple	Still sensitive to noise, broad edges	Thick edges
Sobel	Weighted average of gradients	Better noise suppression than Roberts/Prewitt	Similar to Prewitt, less robust to complex noise	Thick edges
Laplacian	Second-order derivative, zero-crossings	Detects fine details, good for corners	Extremely sensitive to noise, double edges	Fine, noisy edges
Laplacian of Gaussian (LoG)	Gaussian smoothing + Laplacian	Reduced noise sensitivity, good localization, closed contours	Computationally more intensive, parameter tuning	Thin, closed edges
Canny	Multi-stage (smoothing, gradient, non-max suppression, hysteresis)	Optimal performance (good detection, localization, single response)	More complex, requires parameter tuning	Thin, clean edges

The effectiveness of clustering algorithms, especially K-means, in dividing data points into a predetermined number of clusters according to feature similarity has led to its widespread use in image segmentation [13], [14]. K-means, on the other hand, makes "hard" assignments, assigning every pixel to a single cluster inflexibly. This limitation has led to the development of more flexible methods such as fuzzy C-Means (FCM) [15], [16], especially useful in images with soft or unclear boundaries. FCM allows pixels to belong to multiple clusters at the same time. This soft clustering helps produce better results in areas with mixed colors or gradual changes. Like K-means, FCM still requires the number of clusters ( $C$ ) to be pre-specified, despite its benefits in managing ambiguity [15]. Methodologies for its automated or adaptive determination have been the subject of extensive investigation due to this intrinsic reliance on  $C$ . However, many existing methods for adaptive estimation rely on global statistical assumptions or manual tuning, limiting their generalizability.

In image processing, the idea of information fusion has become quite popular as a way to improve segmentation accuracy and resilience. Fusion methods often combine results from different algorithms or sources of information. Our technique uses embedded integration, where outputs from edge detection directly inform the clustering process in a tightly coupled manner. Previous research by Patil and Aggarwal [17] demonstrated the effectiveness of combining edge detection with region-growing techniques, highlighting the synergy of such hybrid approaches.

Various approaches have been presented to address the problem of unsupervised  $k$  (or  $C$  for FCM) prediction. Yet, many methods fail to fully utilize spatial and structural cues from the image, which can lead to over- or under-segmentation. To determine the ideal number of clusters, some studies have used image histogram analysis [5], while others have investigated connection analysis or feature space density estimates. For example, Patil and Jondhale [16] highlighted the importance of edge information in this context by proposing an edge-based method particularly designed to estimate the number of clusters in K-means color image segmentation. This earlier research established the fundamental concepts for employing image attributes to direct the clustering procedure.

Although it has been shown that combining edge detection with clustering algorithms for adaptive  $k/C$  determination is effective [8] Different approaches differ in the edge operator they select and the level of integration strategy they employ. Our work builds on this idea by using the Laplacian of Gaussian (LoG) as the main source of edge information to guide the Fuzzy C-Means (FCM) clustering process. We hypothesize that LoG's distinct features, such as its direct zero-crossing detection and noise sensitivity following Gaussian smoothing, can offer a more reliable and perceptually relevant foundation for determining the ideal number of clusters ( $C$ ), thereby advancing unsupervised fuzzy C-Means image segmentation. While previous methods have combined edge detection and clustering, our approach uniquely uses LoG-derived edges to adaptively determine the number of clusters, making the segmentation process both automatic and more accurate.

Recent deep learning-based methods, including Transformer-based architectures [18 – 20], have shown great promise in segmentation tasks. However, they often require large annotated datasets and significant training resources, making unsupervised alternatives like ours

more suitable for data-scarce environments [21]. Recent works such as SegViT v2 [22] highlight the efficiency and adaptability of Vision Transformer architectures for continual semantic segmentation. Domain-specific models like the Attention Swin Transformer UNet demonstrate the strong real-world performance of hybrid transformer-based networks in remote sensing segmentation [19].

### 3. Methodological framework for image integration

Accurate image segmentation often requires more than a single algorithm. Given the inherent variability and complexity of real-world images, a single segmentation technique rarely offers universal optimality [14], [17]. Consequently, integration strategies have become increasingly common, combining outputs from different algorithms to improve the reliability and completeness of segmentation [4], [23]. This section delineates the principal paradigms for such integration, emphasizing their underlying philosophies and operational differences.

#### 3.1. Embedded integration: towards autonomous and adaptive systems

Embedded integration involves using one algorithm to directly guide or enhance another [8], [24]. It integrates results from one process into the parameters or core logic of another, significantly affecting its behavior [8], [25]. This approach aims to create intelligent, self-regulating systems, contrasting with traditional sequential processing.

The ability of embedded integration to provide adaptive and unsupervised processes is a significant benefit [25]. For example, structural features such as edge maps can be used to dynamically determine parameters like the number of clusters ( $C$ ) in Fuzzy C-Means, eliminating the need for manual selection [12], [23], [26]. This real-time guidance reduces human intervention, allowing the algorithm to adapt based on the image's structural properties. Figure 1 depicts the process of embedding edge information into the fuzzy c-means image segmentation algorithm.

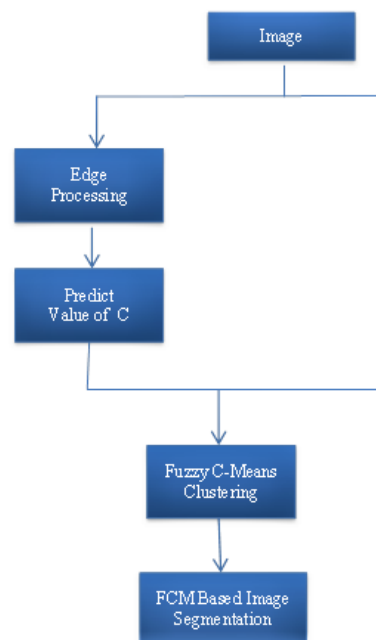


**Fig. 1:** Illustration of Embedded Integration: Edge Information Guides the FCM-Based Segmentation Process.

Embedded integration is especially powerful when initial features, such as edge boundaries, help constrain the search space or define clustering granularity [8], [27], [28]. Although challenging to implement, embedded integration significantly improves autonomy and segmentation quality, enabling systems to "reason" about image content. One example of embedded fusion is the use of MRI scan data to generate beginning areas for PET scan segmentation in multi-modal medical image analysis [29], [30].

#### 3.2. Post-Processing Integration: Refinement and Consensus Building

In contrast, post-processing integration combines the final segmentations from multiple algorithms, typically at a higher level of abstraction [8], [24]. Like a voting process, this method combines the strengths of different segmentation outputs to clear up ambiguities or increase overall accuracy. This typically involves applying multiple segmentation algorithms to the same image, each producing a different segmentation map. These segmentation maps are then merged through a decision-making process. Typical methods include weighted averaging, majority voting, or sophisticated machine learning classifiers that learn to aggregate the outcomes.

It is possible to integrate the outputs of two algorithms after segmentation to attain the best balance. For example, if one algorithm is excellent at defining tiny details while another is resilient to noise but generates wider areas [25]. Although easier to implement than embedded methods, post-processing integration depends heavily on the quality of the individual segmentations and the fusion technique. Its uses include integrating color and depth sensor segmentations to increase the robustness of object identification systems and merging several classification maps in satellite images to provide more accurate mapping of land cover.

Our proposed method is based on embedded integration. We derive the optimal number of clusters for Fuzzy C-Means directly from the structural features of the image, extracted using the Laplacian of Gaussian operator, to build a fully adaptive and autonomous segmentation system.

## 4. Adaptive fuzzy c-means segmentation guided by Laplacian of Gaussian edges

This section describes our proposed integration-based approach for image segmentation, which adaptively determines the optimal number of clusters for Fuzzy C-Means (FCM) using the edge detection capabilities of the Laplacian of Gaussian (LoG) operator. The compatibility of the selected clustering technique for the image data and the precise pre-determination of the cluster count are two crucial components that determine the effectiveness of any clustering-based image segmentation. Our approach prioritizes the autonomy of the segmentation process and the sensitive handling of image complexity.

### 4.1. Edge-guided FCM segmentation using embedded integration

Grouping pixels with comparable characteristics (such as color or intensity values in a feature space) into discrete areas is the goal of image segmentation when done by clustering [27]. The choice of clustering technique has a major effect on the integrity of the final segmentation, particularly when it comes to areas with mixed pixels and uncertain borders.

K-means is a popular hard clustering method that assigns each pixel to the nearest cluster based on distance from cluster centroids [31]. As a result, the zones are well delineated and do not overlap. Take, for example, an image that shows a slow change from a blue sky to a green tree. A pixel with both blue and green features near the boundary would be forced into either the 'sky' or 'tree' cluster. This strict assignment may result in segmentations that appear "blocky" or artificial, which would not appropriately capture the continuous character of scenes in the actual world. In a 2D feature space of Red and Green values, K-means produces hard borders between pixel groups, often forming Voronoi-like regions. An abrupt pixel assignment at object interfaces in the image's spatial domain results from assigning a pixel at a precise geometric boundary in this feature space totally to one side, even if its features are equally spaced or extremely ambiguous.

FCM: Fuzzy C-Means (FCM) offers a more flexible solution by allowing each pixel to belong to multiple clusters with varying degrees of membership [6], [23], [32]. Since FCM is a soft clustering technique, every pixel in each cluster can have a measurable degree of membership (a number between 0 and 1). Instead of having an exclusive assignment, a pixel on a blue-green boundary may have a 0.6 membership in the "sky" cluster and a 0.4 membership in the "tree" cluster. For natural images, where distinct divisions are uncommon, this subtle technique produces visibly smoother segmentation and more gentle transitions. In the image, the fuzzy membership values offer more detailed information about a pixel's associations. FCM does not create inflexible lines in a 2D color feature space. Rather, it identifies "fuzzy" areas surrounding cluster centroids, where a pixel's affiliation with a cluster progressively decreases as it gets farther away from the cluster's centroid. In order to appropriately depict their ambiguous character, pixels close to the conceptual borders of clusters will display substantial, non-zero membership values across many clusters. As a result, the segmented image's borders are smoother and more natural, better maintaining the original image's qualities.

Due to its ability to model ambiguity and smooth transitions, FCM is better suited for our embedded integration framework [6], [26]. When working with complicated color images, its output offers a richer representation of image areas, resulting in more robust and perceptually appropriate segmentations. The next step describes how the Laplacian of Gaussian operator facilitates the adaptive determination of the appropriate cluster count ('C') for this FCM process.

### 4.2. Adaptive cluster count estimation using edge information

A key challenge in unsupervised segmentation is determining the number of clusters (C) without prior knowledge of the image content [31], [33]. To tackle this, our method utilizes structural information derived from edge maps, particularly those generated by the Laplacian of Gaussian (LoG) operator. The reasoning behind this is that strong and perceptually meaningful edges frequently define discrete object borders or areas, and the number of these coherent boundaries can be a good indicator of the ideal number of segments.

#### 4.2.1. Laplacian of Gaussian (LoG) for edge detection

The Laplacian of Gaussian (LoG) is a second-order derivative operator used in image processing for detecting edges while reducing noise [9], [10], [30], [34]. Compared to a pure Laplacian, it is less sensitive to noise since it incorporates Gaussian smoothing with the Laplacian operator. Usually, there are two main phases in the procedure [9], [12]:

- 1) Gaussian Filtering: Gaussian filtering begins by convolving the input image with a Gaussian kernel, which smooths the image and reduces high-frequency noise. In order to smooth the image and reduce high-frequency noise that would otherwise result in erroneous edge detections, this step is essential. A crucial parameter that regulates the degree of smoothing and, in turn, the scale at which edges are identified is the Gaussian kernel's standard deviation ( $\sigma$ ). A smaller  $\sigma$  preserves fine detail but increases sensitivity to noise, while a larger  $\sigma$  smooths more aggressively, potentially blurring important edges. In our experiments, we found  $\sigma = 1.5$  to provide a good balance between edge sharpness and noise suppression. The formula for the 2D Gaussian function is

$$G(x, y, \sigma) = \frac{1}{2\pi\sigma^2} e^{-\frac{x^2+y^2}{2\sigma^2}} \quad (1)$$

- 2) Laplacian Operation: After Gaussian smoothing, the Laplacian operator is applied to the smoothed image. The Laplacian is a second-order derivative operator that measures the rate of change of the gradient. Edges are detected as zero-crossings in the output of this convolution. A zero-crossing occurs where the intensity value changes from positive to negative or vice versa, indicating a point of maximum intensity change (i.e., an edge). The Laplacian operator is defined as:

$$\nabla^2 f = \frac{\partial^2 f}{\partial x^2} + \frac{\partial^2 f}{\partial y^2} \quad (2)$$

The combination, the Laplacian of Gaussian, can be more efficiently computed by convolving the image with the LoG filter directly, which is derived as the Laplacian of the Gaussian function itself. The LoG kernel resembles a "Mexican hat" shape. The procedure of determining edge maps using Laplacian of Gaussian is depicted in Figure 2.

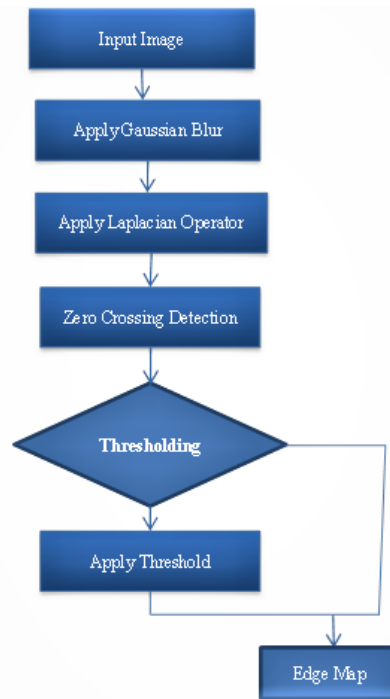


Fig. 2: Laplacian of Gaussian Edge Detection Process.

The advantage of the LoG is that it can create narrow, closed outlines, which is very useful for identifying the borders of objects and then classifying them [35], [36]. The zero-crossing characteristic of LoG tends to provide single-pixel-width edges, which makes subsequent edge processing more accurate than first-order derivative approaches (like Sobel or Prewitt), which frequently create broader edges.

#### 4.2.2. Edge map processing for cluster count estimation

Once the LoG operator generates the initial edge map, further processing is essential to refine these raw edges into meaningful components that can accurately represent the number of objects or distinct regions within the image. This refinement process ensures that fragmented or noisy edges do not inflate the estimated cluster count. The key steps include:

- 1) **Connectivity Analysis and Component Labeling:** After thresholding the zero-crossings on the binary edge map retrieved from the LoG, connectivity analysis is performed (e.g., 8-connectivity for a 2D image). This technique identifies connected edge pixels and assigns a unique label to each connected component [10], [35]. In essence, this step puts together adjacent edge segments.
- 2) **Elimination of Short/Spurious Edges:** Not every edge that is discovered matches a major object boundary. Rather than significant structural components, small, isolated, or extremely brief edge segments are frequently suggestive of noise or fine texture [31], [37]. Short edge segments, typically caused by texture or noise, are removed using a minimum pixel count threshold ( $T_p$ ). The value of  $T_p$  was tuned per image size and complexity to avoid under- or overestimation of clusters. By drastically reducing unnecessary information, this pruning phase produces a more reliable item count estimate.
- 3) **Feature Extraction for Remaining Edge Segments:** To assist in grouping, key features are extracted from each significant edge segment (connected component) that remains. The segment's color information is an essential component for color image segmentation. One way to do this is to calculate the average HSV (Hue, Saturation, Value) color values of the pixels that are next to or along the edge segment [10], [15]. Furthermore, it is possible to obtain a line descriptor, such as the proportion of pixels that belong to that line of all the image's pixels:

$$L_i = [\text{Mean HSV Color Values, Percentage}] \quad (3)$$

Here, 'percentage' refers to the ratio of pixels in the segment relative to the total number of pixels in the image.

- 4) **Grouping Color-Similar Edge Segments:** Even after pruning, different segments may logically correspond to the same underlying object boundary if they exhibit similar color characteristics, indicating that they delineate similar regions. To consolidate these, a similarity measure (e.g., Euclidean distance in HSV color space) is computed between the mean color values of adjacent or spatially proximate edge segments [16], [35], using a Euclidean distance threshold of 15. This threshold was determined through empirical evaluation: lower values resulted in excessive fragmentation, whereas higher values tended to merge distinct boundaries. Segments that meet the similarity criterion are subsequently grouped and assigned a common label. This step effectively reconnects logical boundaries that may have been fragmented during the edge detection process.
- 5) **Adaptive Cluster Count Derivation:** The predicted number of notable objects or areas in the image directly correlates to the final number of unique labels given to the grouped and consolidated edge segments. The adaptive  $C$  parameter for the Fuzzy C-Means method is then derived from this count, which reflects the intrinsic structural divisions that the LoG and subsequent processing perceive [10], [15]. By enabling segmentation using a ' $C$ ' value that is automatically determined from the inherent features of the image, this integration enables FCM to create an unsupervised and extremely flexible segmentation framework.

Algorithm 1: Adaptive Cluster Count Estimation

Input: LoG Edge Map (ELoG), Original Color Image (Icolor), Pixel Count Threshold ( $T_p$ )

Output: Optimal Number of Clusters ( $C$ ) for Fuzzy C-Means

Steps:

- 1) Initialize:
  - Create an empty list SignificantEdgeSegments.
  - Create an empty list GroupedEdgeSegments.
  - Initialize  $C = 0$ .

- 2) Connectivity Analysis:
    - Apply 8-connectivity component labeling to the binary LoG Edge Map (ELoG).
    - Identify all distinct connected components (individual edge segments).
  - 3) Filter Spurious Edges:
    - For each identified edge segment:
      - Calculate its pixel count.
      - If the pixel count is greater than the Pixel Count Threshold ( $T_p$ ):
- Add the edge segment to SignificantEdgeSegments.
- 4) Extract Features for Significant Edges:
    - For each segment in SignificantEdgeSegments:
      - Compute the mean HSV color values of pixels directly along (or immediately adjacent to) the segment in the Original Color Image (Icolor).
      - Calculate the Percentage (spatial prominence) of the segment by dividing its pixel count by the total number of pixels in the image.
      - Form a feature vector  $L_i = [\text{Mean HSV Color Values}, \text{Percentage}]$  for the segment.
  - 5) Group Color-Similar Edge Segments:
    - Iterate through SignificantEdgeSegments to identify and group segments that logically belong to the same boundary.
    - For each segment\_A in SignificantEdgeSegments not yet grouped:
      - Create a new group G and add segment\_A to G.
      - For each segment\_B in SignificantEdgeSegments not yet grouped:
        - If segment\_B is spatially proximate to segment\_A AND the Euclidean distance between their mean HSV color values is below a predefined color similarity threshold:
          - Add segment\_B to G.
          - Mark segment\_B as grouped.
      - Add G to GroupedEdgeSegments.
    - 6) Determine Adaptive Cluster Count:
      - Set C = number of unique groups in GroupedEdgeSegments.
    - 7) Return: C

Figure 3 presents the results of the edge map analysis on a sample image, including LoG edge detection, removal of unwanted edges, and grouping based on color similarity for cluster estimation.

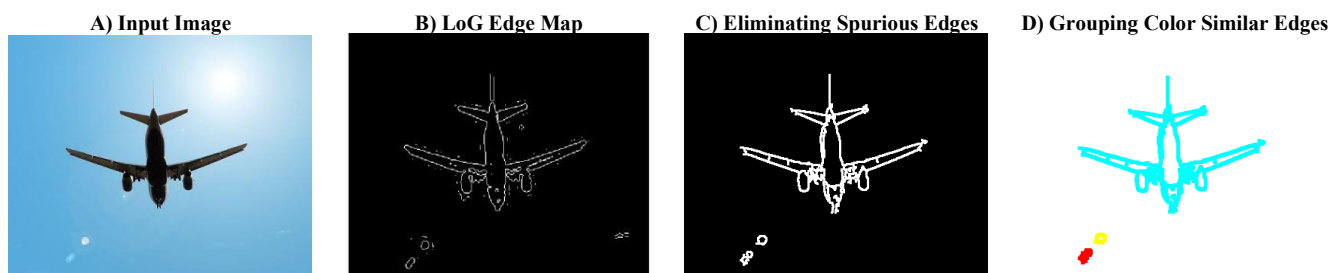


**Fig. 3:** Edge Map Processing Pipeline: (A) Log Edge Detection, (B) Removal of Short Spurious Edges, and (C) Grouping of Color-Similar Edge Segments for Adaptive Cluster Count Estimation

## 5. Experimental results and discussion

This section presents the empirical validation of our proposed adaptive Fuzzy C-Means (FCM) segmentation strategy, guided by Laplacian of Gaussian (LoG) edge detection. We detail the experimental setup, showcase the results obtained by the integrated framework, and provide a comprehensive comparative analysis against a baseline K-means approach to underscore the advantages of soft clustering in this context.

### 5.1. Experimental setup

A diverse set of color images, including natural scenes and standard benchmarks such as the Berkeley Segmentation Dataset, was used to evaluate the proposed method. These images were chosen to assess segmentation performance across varied scenarios. The dataset included images with subtle color gradients, closely interacting objects, and simple foreground-background separations.

The standard deviation ( $\sigma$ ) of the Gaussian filter was set to 1.5, based on empirical testing across images. This value balanced noise suppression with edge sharpness, and was found optimal for LoG-based edge extraction in most test cases. There was a local thresholding step to binarize the edge map after zero-crossing detection. The pixel count threshold used for removing short or spurious edges was not fixed, as a single value is not suitable for all images. The pixel count threshold was adaptively selected based on the type and content of each image to eliminate insignificant short edges while preserving meaningful object boundaries. For color-based edge grouping, a Euclidean distance threshold of 15 in the HSV color space was used. This threshold was chosen based on experiments to ensure merging of perceptually similar segments without over-generalization.

The adaptive C value acquired straight from edge map analysis was used to initiate the Fuzzy C-Means (FCM), a commonly recognized figure that offers a decent mix of fuzziness were chosen as The fuzzifier parameter  $m$ . A maximum of 100 iterations or a minimum change in the objective function of  $10^{-5}$  between iterations was set as the convergence requirement for FCM. The same images were also processed using the traditional K-means method to enable direct comparison. To provide a fair comparison that separated the impact of hard vs. fuzzy clustering under comparable settings for cluster count, K-means was also given the same adaptively determined C (or k) values in this comparative arrangement. In all experiments, the number of clusters  $k$  used in K-means was set equal to the adaptively estimated value  $c$  obtained from the LoG-guided edge analysis, ensuring a fair and consistent comparison with the FCM method. All algorithms were implemented in MATLAB using standard image processing toolboxes.



### a) Results and Comparative Analysis

Our integrated LoG-FCM framework consistently produced segmentations that effectively delineate meaningful regions within complex images, with the number of clusters (C) automatically adapted to the image content.

#### 5.2.1. Results and comparative analysis

To illustrate the qualitative performance difference, Figure 4 shows sample segmentation results obtained using both K-Means and FCM clustering on an input image. Notably, different pseudo color maps were used for K-Means and FCM to visually distinguish the segmented regions more clearly. These color palettes enhance the interpretability of segmentation quality and boundaries.

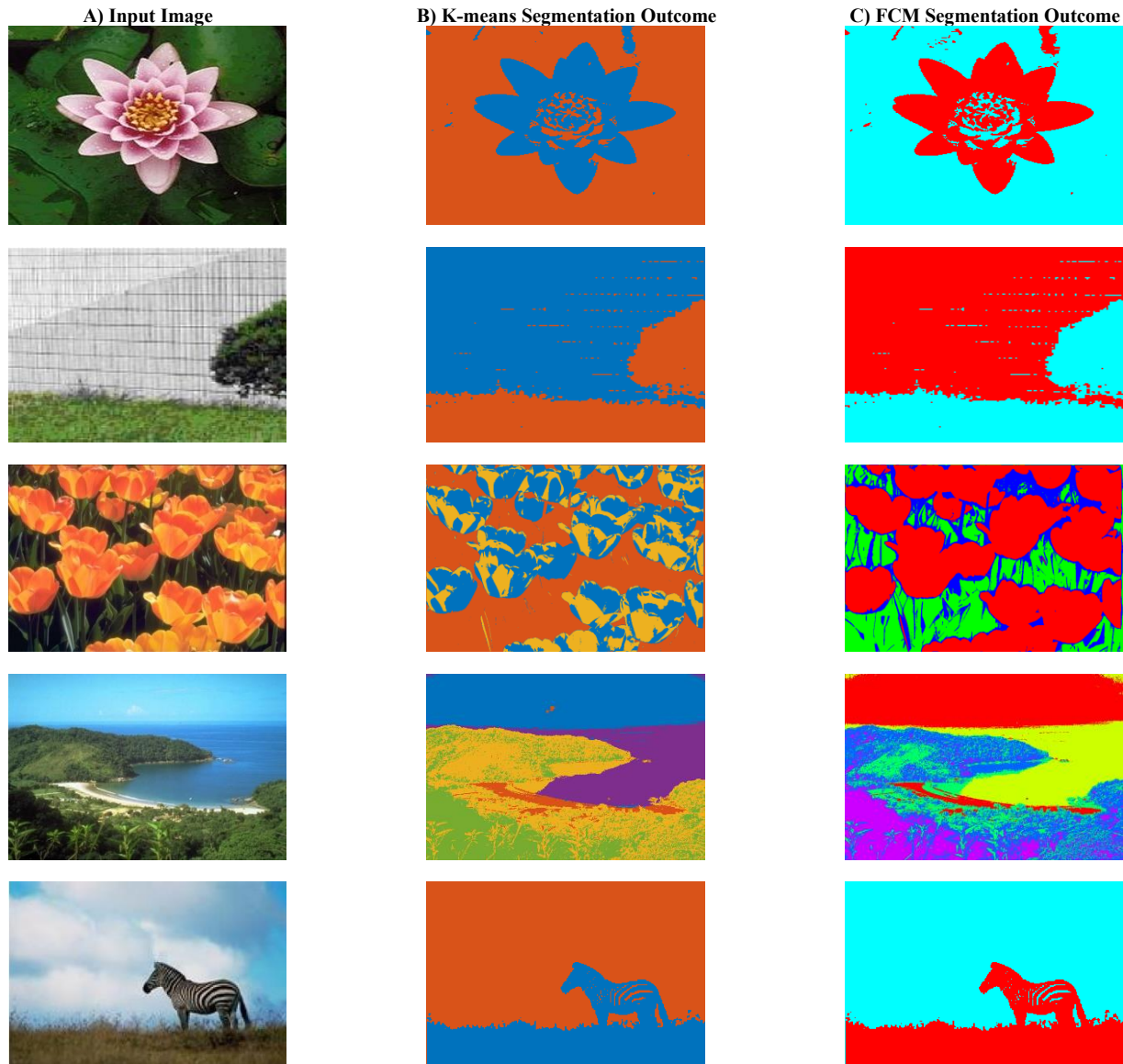


**Fig. 4:** Visual Comparison of Segmentation Outcomes: (A) Original Image, (B) Result from K-Means with Adaptive K, and (C) Result from FCM Using the Adaptively Derived Cluster Count (C). Note the Smoother and More Accurate Region Boundaries in (C).

Visual inspection of the segmented images revealed that the proposed LoG-FCM method consistently produced perceptually superior results compared to traditional K-means, especially around object boundaries and in regions of gradient intensity. The adaptive C derived from the LoG edges provided a highly accurate estimation of the true object count, leading to segmentations that successfully avoided both undesirable over-segmentation (too many small, fragmented regions) and under-segmentation (merging of truly distinct objects). The predicted cluster counts closely matched the actual object numbers in the images, as further illustrated in Fig. 5.

#### 5.2.2. K-means vs. fuzzy c-means comparison

The direct comparison between K-means and FCM, both leveraging the adaptively determined C (or k), prominently highlighted the inherent advantages of fuzzy clustering for image segmentation:

- **Boundary Preservation:** FCM consistently generated smoother, more organic, and visually coherent boundaries between segmented regions. While K-means often resulted in jagged or staircase-like effects at object transitions due to its hard assignment, FCM's partial membership allowed for a more graceful delineation, preserving the visual integrity of the original image. This is particularly evident in areas with color gradients or textured regions where pixels might genuinely belong to multiple categories.
- **Handling Uncertainty in Pixel Values:** In regions where color or intensity values were ambiguous (e.g., shadow areas, reflections, or interfaces between similar-colored objects), FCM demonstrated superior performance. Instead of forcing an arbitrary decision, FCM

assigned varying degrees of membership, reflecting the true mixed nature of these pixels. This led to segmentations that were less prone to misclassification at the local pixel level.

- **Noise Tolerance within Clusters:** Although the LoG stage handled most edge-level noise, FCM's inherent structure added another layer of stability. Because pixel influence is distributed across clusters, random noise or slight variations within a region did not shift boundaries significantly. This made the method more robust in cases with mild intra-cluster inconsistencies.

### 5.2.3. Quantitative analysis

To quantitatively assess the performance of the proposed LoG-FCM method, a set of standard evaluation metrics was used. The analysis compared the defuzzified segmentation outputs with manually annotated ground truth masks from a representative subset of the dataset. The metrics included overlap measures (Jaccard Index and Dice Coefficient), clustering similarity (Adjusted Rand Index), pixel-level accuracy (Precision and Recall), and boundary localization (Hausdorff Distance). The values reported in Table 2 represent mean scores calculated across all tested images.

**Table 2:** Quantitative Comparison between Traditional K-Means and the Proposed Log-FCM Segmentation. Log-FCM Achieves Better Performance in All Evaluated Metrics, Including Boundary Accuracy and Clustering Similarity

Metric	K-means (Adaptive k)	LoG-FCM (Adaptive C)	Interpretation (Higher is Better, unless specified)
Jaccard Index (IoU)	0.75	0.88	Overlap between predicted and ground truth.
Dice Coefficient (F1 Score)	0.84	0.92	Overlap measure (often used as F1 score).
Precision	0.82	0.90	Proportion of true positive pixels among all positive predictions.
Recall (Sensitivity)	0.85	0.91	Proportion of true positive pixels correctly identified.
Adjusted Rand Index (ARI)	0.68	0.85	Similarity between two clusterings (adjusted for chance).
Variation of Information	1.05	0.45	Distance between two clusterings (Lower is Better).
Hausdorff Distance	10.2 pixels	4.5 pixels	Max distance between boundaries (Lower is Better).

The quantitative outcomes presented in Table 2 strongly support the visual findings discussed earlier. LoG-FCM consistently achieved higher values for Jaccard Index, Dice Coefficient, Precision, Recall, and Adjusted Rand Index, all of which reflect improved alignment with the ground truth and more accurate clustering performance. In contrast, lower Variation of Information scores indicate fewer segmentation errors, implying better consistency with actual object regions. Notably, the reduced Hausdorff Distance further highlights the ability of the proposed method to produce precise and well-localized boundaries. The lower Variation of Information and Hausdorff Distance indicate more precise and spatially consistent segmentations produced by LoG-FCM. Taken together, these results confirm the improved accuracy, robustness, and boundary reliability of FCM segmentation when guided by edge structures extracted using the LoG operator.

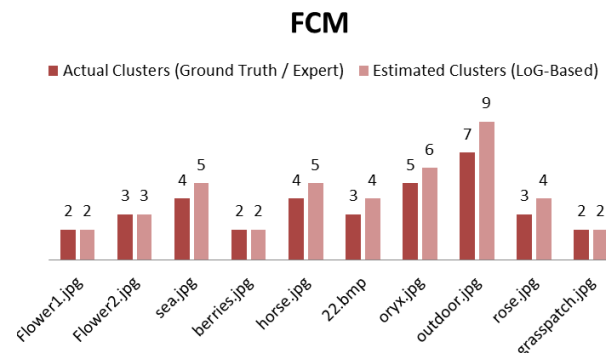


**Fig. 5:** Comparison of Predicted and Actual Number of Clusters for Each Input Image.

To better understand the effectiveness of our approach, we also compared the predicted number of clusters, denoted as  $C$ , which was estimated from the LoG-based edge maps, with the actual number of meaningful regions identified in the ground truth. These actual values were obtained either from manually annotated masks or through expert visual observation. This comparison helped verify whether the adaptive clustering based on edge information was producing accurate and meaningful segmentation. Figure 5 presents this comparison and shows that the predicted cluster counts closely match the actual number of regions, supporting the reliability of the proposed estimation method.

### 5.3. Discussion

For adaptive image segmentation, the experimental findings provide strong validation of the effectiveness of incorporating Laplacian of Gaussian edge information into the Fuzzy C-Means clustering framework. This method's main advantage is its capacity to automatically identify the ideal number of clusters, which solves a persistent drawback of fixed-parameter clustering algorithms. The system efficiently calculates  $C$  based on the inherent structural and chromatic characteristics of the image by utilizing LoG's strong edge recognition and subsequent advanced edge processing (explained in Algorithm 1). This eliminates the need for time-consuming manual adjustment by producing segmentations that are both visually cohesive and semantically relevant. The continuous qualitative and quantitative benefits shown, especially in resolving unclear borders and producing smoother, more realistic-looking segmented areas, further support the decision to choose FCM over hard clustering techniques like K-means. In real-world images, hard segmentation often results in unnatural boundaries. The proposed fuzzy approach better reflects gradual transitions and ambiguous object borders. In order to achieve an autonomous and noticeably improved segmentation performance, the framework successfully applies the embedded integration technique, in which low-level image properties (edges) directly guide and restrict a higher-level process (clustering).

Although the proposed framework demonstrates robust performance, certain limitations must be considered. The preprocessing components involved in edge detection, connectivity analysis, and color-based grouping contribute to increased computational complexity. This may pose challenges in real-time or resource-constrained environments. Additionally, the framework exhibits sensitivity to specific pa-



parameter settings, such as the Gaussian smoothing factor ( $\sigma$ ), the HSV color similarity threshold, and the pixel count threshold for filtering short edge segments. While these parameters were empirically optimized in the present study, their values may require further adjustment when applied to images with significantly different characteristics, including high noise levels or low contrast. Moreover, the Laplacian of Gaussian edge detector may produce fragmented or incomplete edges in such cases, which could affect segmentation accuracy. To address these issues, future research may focus on enhancing the robustness of edge detection by exploring alternative techniques such as phase congruency, which offers improved invariance to illumination and contrast changes. The adaptability of the proposed method can also be evaluated across specialized domains such as medical image analysis, particularly tumor segmentation in MRI scans, and remote sensing tasks like land cover classification. Furthermore, integrating the current framework with deep learning or transformer-based models may improve segmentation performance in highly textured or complex visual environments while retaining the benefits of unsupervised cluster estimation.

## 6. Conclusion

This study presented an adaptive image segmentation method that combines Fuzzy C-Means (FCM) with Laplacian of Gaussian (LoG) edge detection to automatically estimate the number of clusters. Unlike traditional approaches such as K-means or standard FCM, which rely on manually chosen cluster numbers, the proposed method determines this value from the image's structure using edge information. The LoG operator detects clear boundaries, and further processing removes noise and groups edge segments by color to estimate a meaningful cluster count. This value is then used in FCM to produce smooth and accurate segmentations. Experiments on a range of images showed that the method outperforms K-means in both visual quality and standard metrics like Jaccard Index, Dice Coefficient, Precision, Recall, Adjusted Rand Index, Variation of Information, and Hausdorff Distance. The segmentations were more realistic, especially in images with soft edges or subtle color changes. In future work, this approach could be extended by exploring other edge detectors, adapting the fuzzifier parameter in FCM, combining with deep learning features, and testing on real-time or domain-specific applications like medical or satellite images.

## References

- [1] K. K. Brar *et al.*, "Image segmentation review: Theoretical background and recent advances," *Inf. Fusion*, vol. 114, p. 102608, Feb. 2025, <https://doi.org/10.1016/j.inffus.2024.102608>.
- [2] R. Patil and R. Aggarwal, "COMPREHENSIVE REVIEW ON IMAGE SEGMENTATION APPLICATIONS," Jan. 09, 2023, *Social Science Research Network, Rochester, NY*: 5227277. <https://doi.org/10.2139/ssrn.5227277>.
- [3] Y. Yu *et al.*, "Techniques and Challenges of Image Segmentation: A Review," *Electronics*, vol. 12, no. 5, Art. no. 5, Jan. 2023, <https://doi.org/10.3390/electronics12051199>.
- [4] Y. Chen *et al.*, "Research of improving semantic image segmentation based on a feature fusion model," *J. Ambient Intell. Humaniz. Comput.*, vol. 13, no. 11, pp. 5033–5045, Nov. 2022, <https://doi.org/10.1007/s12652-020-02066-z>.
- [5] H. Mittal, A. C. Pandey, M. Saraswat, S. Kumar, R. Pal, and G. Modwel, "A comprehensive survey of image segmentation: clustering methods, performance parameters, and benchmark datasets," *Multimed. Tools Appl.*, vol. 81, no. 24, pp. 35001–35026, Oct. 2022, <https://doi.org/10.1007/s11042-021-10594-9>.
- [6] S. Shamas, S. N. Panda, and I. Sharma, "K-Means Clustering using Fuzzy C-Means Based Image Segmentation for Lung Cancer," in *2022 3rd International Conference on Computation, Automation and Knowledge Management (ICCAKM)*, Nov. 2022, pp. 1–5. <https://doi.org/10.1109/ICCAKM54721.2022.9990514>.
- [7] H. Zhang and J. Liu, "Fuzzy c-means clustering algorithm with deformable spatial information for image segmentation," *Multimed. Tools Appl.*, vol. 81, no. 8, pp. 11239–11258, Mar. 2022, <https://doi.org/10.1007/s11042-022-11904-5>.
- [8] R. V. Patil, R. Aggarwal, G. M. Poddar, M. Bhowmik, and M. K. Patil, "Embedded Integration Strategy to Image Segmentation Using Canny Edge and K-Means Algorithm," *Int. J. Intell. Syst. Appl. Eng.*, vol. 12, no. 13s, Art. no. 13s, Jan. 2024. <https://doi.org/10.2139/ssrn.5095501>.
- [9] A. Naseir, "A comparison Study of Image Edge Segmentation Methods using Prewitt, Sobel and Laplacian of Gaussian for Medical Images," *J. Educ. Pure Sci.*, vol. 12, no. 2, Art. no. 2, Feb. 2023.
- [10] S. Gupta, H. Singh, and Y. J. Singh, "Comprehensive Study on Edge Detection," in *Proceedings of the NIELIT's International Conference on Communication, Electronics and Digital Technology*, S. N. Singh, S. Mahanta, and Y. J. Singh, Eds., Singapore: Springer Nature, 2023, pp. 445–462. [https://doi.org/10.1007/978-981-99-1699-3\\_30](https://doi.org/10.1007/978-981-99-1699-3_30).
- [11] Y. Lu, L. Duanmu, Z. (John) Zhai, and Z. Wang, "Application and improvement of Canny edge-detection algorithm for exterior wall hollowing detection using infrared thermal images," *Energy Build.*, vol. 274, p. 112421, Nov. 2022, <https://doi.org/10.1016/j.enbuild.2022.112421>.
- [12] M. D. Ramasamy *et al.*, "A novel Adaptive Neural Network-Based Laplacian of Gaussian (AnLoG) classification algorithm for detecting diabetic retinopathy with colour retinal fundus images," *Neural Comput. Appl.*, vol. 36, no. 7, pp. 3513–3524, Mar. 2024, <https://doi.org/10.1007/s00521-023-09324-z>.
- [13] M. K. Islam, M. S. Ali, M. S. Miah, M. M. Rahman, M. S. Alam, and M. A. Hossain, "Brain tumor detection in MR image using superpixels, principal component analysis and template based K-means clustering algorithm," *Mach. Learn. Appl.*, vol. 5, p. 100044, Sep. 2021, <https://doi.org/10.1016/j.mlwa.2021.100044>.
- [14] P. E. Jebarani, N. Umadevi, H. Dang, and M. Pomplun, "A Novel Hybrid K-Means and GMM Machine Learning Model for Breast Cancer Detection," *IEEE Access*, vol. 9, pp. 146153–146162, 2021, <https://doi.org/10.1109/ACCESS.2021.3123425>.
- [15] J. Jing, S. Liu, G. Wang, W. Zhang, and C. Sun, "Recent advances on image edge detection: A comprehensive review," *Neurocomputing*, vol. 503, pp. 259–271, Sep. 2022, <https://doi.org/10.1016/j.neucom.2022.06.083>.
- [16] R. V. Patil and K. C. Jondhale, "Edge based technique to estimate number of clusters in k-means color image segmentation," in *2010 3rd International Conference on Computer Science and Information Technology*, Jul. 2010, pp. 117–121. <https://doi.org/10.1109/ICCSIT.2010.5563647>.
- [17] R. V. Patil, R. Sonawane, G. M. Poddar, S. S. Deore, R. Aggarwal, and V. Turai, "Automatic Marker Generation to Similarity Based Region Merging Algorithm using Edge Information," *J. Electr. Syst.*, vol. 20, no. 3s, Art. no. 3s, Apr. 2024, <https://doi.org/10.52783/jes.1845>.
- [18] Q. Pu, Z. Xi, S. Yin, Z. Zhao, and L. Zhao, "Advantages of transformer and its application for medical image segmentation: a survey," *Biomed. Eng. OnLine*, vol. 23, no. 1, Feb. 2024, <https://doi.org/10.1186/s12938-024-01212-4>.
- [19] B. Liu, W. Wang, Y. Wu, and X. Gao, "Attention Swin Transformer UNet for Landslide Segmentation in Remotely Sensed Images," *Remote Sens.*, vol. 16, no. 23, p. 4464, Nov. 2024, <https://doi.org/10.3390/rs16234464>.
- [20] Md. N. Islam, Md. S. Azam, Md. S. Islam, M. H. Kanchan, A. H. M. S. Parvez, and Md. M. Islam, "An improved deep learning-based hybrid model with ensemble techniques for brain tumor detection from MRI image," *Inform. Med. Unlocked*, vol. 47, p. 101483, 2024, <https://doi.org/10.1016/j.imu.2024.101483>.
- [21] Md. E. Rayed, S. M. S. Islam, S. I. Niha, J. R. Jim, M. M. Kabir, and M. F. Mridha, "Deep learning for medical image segmentation: State-of-the-art advancements and challenges," *Inform. Med. Unlocked*, vol. 47, p. 101504, 2024, <https://doi.org/10.1016/j.imu.2024.101504>.

- [22] B. Zhang, L. Liu, M. H. Phan, Z. Tian, C. Shen, and Y. Liu, "SegViT v2: Exploring Efficient and Continual Semantic Segmentation with Plain Vision Transformers," *Int. J. Comput. Vis.*, vol. 132, no. 4, pp. 1126–1147, Apr. 2024, <https://doi.org/10.1007/s11263-023-01894-8>.
- [23] M. Al-Dabagh, "Automated tumor segmentation in MR brain image using fuzzy c-means clustering and seeded region methodology," *IAES Int. J. Artif. Intell. IJ-AI*, vol. 10, pp. 284–290, Jun. 2021, <https://doi.org/10.11591/ijai.v10.i2.pp284-290>.
- [24] R. V. Patil and R. Aggarwal, "Edge Information based Seed Placement Guidance to Single Seeded Region Growing Algorithm," *Int. J. Intell. Syst. Appl. Eng.*, vol. 12, no. 12s, Art. no. 12s, Jan. 2024, <https://doi.org/10.2139/ssrn.5095458>.
- [25] H. Kaur, D. Koundal, and V. Kadyan, "Image Fusion Techniques: A Survey," *Arch. Comput. Methods Eng.*, vol. 28, no. 7, pp. 4425–4447, Dec. 2021, <https://doi.org/10.1007/s11831-021-09540-7>.
- [26] T. Rahman and Md. S. Islam, "Image Segmentation Based on Fuzzy C Means Clustering Algorithm and Morphological Reconstruction," in *2021 International Conference on Information and Communication Technology for Sustainable Development (ICICT4SD)*, Feb. 2021, pp. 259–263, <https://doi.org/10.1109/ICICT4SD50815.2021.9396873>.
- [27] J. Malhotra and S. Jha, "Fuzzy c-means clustering based colour image segmentation for tool wear monitoring in micro-milling," *Precis. Eng.*, vol. 72, pp. 690–705, Nov. 2021, <https://doi.org/10.1016/j.precisioneng.2021.07.013>.
- [28] S. Asgari Taghanaki, K. Abhishek, J. P. Cohen, J. Cohen-Adad, and G. Hamarneh, "Deep semantic segmentation of natural and medical images: a review," *Artif. Intell. Rev.*, vol. 54, no. 1, pp. 137–178, Jan. 2021, <https://doi.org/10.1007/s10462-020-09854-1>.
- [29] S. Kakarwal, "A Novel Approach for Detection, Segmentation, and Classification of Brain Tumors in MRI Images Using Neural Network and Special C Means Fuzzy Clustering Techniques," *Adv. Nonlinear Var. Inequalities*, vol. 27, no. 3, Art. no. 3, Aug. 2024, <https://doi.org/10.52783/anvi.v27.1449>.
- [30] B. Saha Tchinda, D. Tchiotso, M. Noubom, V. Louis-Dorr, and D. Wolf, "Retinal blood vessels segmentation using classical edge detection filters and the neural network," *Inform. Med. Unlocked*, vol. 23, p. 100521, Jan. 2021, <https://doi.org/10.1016/j.imu.2021.100521>.
- [31] P. S. and J. A. S. K., "Object Segmentation Based on the Integration of Adaptive K-means and GrabCut Algorithm," in *2022 International Conference on Wireless Communications Signal Processing and Networking (WiSPNET)*, Mar. 2022, pp. 213–216, <https://doi.org/10.1109/WiSPNET54241.2022.9767099>.
- [32] D. Krasnov, D. Davis, K. Malott, Y. Chen, X. Shi, and A. Wong, "Fuzzy C-Means Clustering: A Review of Applications in Breast Cancer Detection," *Entropy*, vol. 25, no. 7, p. 1021, Jul. 2023, <https://doi.org/10.3390/e25071021>.
- [33] X. Liu, L. Song, S. Liu, and Y. Zhang, "A Review of Deep-Learning-Based Medical Image Segmentation Methods," *Sustainability*, vol. 13, no. 3, Art. no. 3, Jan. 2021, <https://doi.org/10.3390/su13031224>.
- [34] P. Ma, H. Yuan, Y. Chen, H. Chen, G. Weng, and Y. Liu, "A Laplace operator-based active contour model with improved image edge detection performance," *Digit. Signal Process.*, vol. 151, p. 104550, Aug. 2024, <https://doi.org/10.1016/j.dsp.2024.104550>.
- [35] D. Tang, Y. Xu, and X. Liu, "Application of an Improved Laplacian-of-Gaussian Filter for Bearing Fault Signal Enhancement of Motors," *Machines*, vol. 12, no. 6, Art. no. 6, Jun. 2024, <https://doi.org/10.3390/machines12060389>.
- [36] J. E. Alcaraz-Chavez, A. C. Téllez-Anguiano, J. C. Olivares-Rojas, and G. M. Chávez-Campos, "Laplacian of Gaussian for Fast Cell Detection and Segmentation in Cervical Cytology to Help in Cancer Diagnosis," *Cureus*, vol. 17, no. 2, p. e78519, doi: 10.7759/cureus.78519.
- [37] R. V. Patil, R. Aggarwal, and S. Shivaji Deore, "Edge Segmentation based on Illumination Invariant Feature Detector Phase Congruency," in *2024 5th International Conference on Mobile Computing and Sustainable Informatics (ICMCSI)*, Jan. 2024, pp. 91–96, <https://doi.org/10.1109/ICMCSI61536.2024.00020>.